Structural and magnetic properties of $HfFe_6Ge_6$-type $ErMn_6Sn_{6-x}Ga_x$ ($x=0-2.0$) compounds

Jin-lei Yao,[1,2,*] Shao-ying Zhang,[1] Juan Du,[3] Mi Yan,[2] De-ren Yang,[2] Li-gang Zhang,[4] Shi-min Liu,[3] and Bao-gen Shen[1]
[1]*State Key Laboratory of Magnetism, Institute of Physics and Center for Condensed Matter Physics, Chinese Academy of Sciences, Beijing 100080, China*
[2]*State Key Laboratory of Silicon Materials, Zhejiang University, Hangzhou 310027, China*
[3]*School of Materials Science and Engineering, Yanshan University, Qinhuangdao 066004, China*
[4]*Department of Applied Physics, University of Science and Technology of Wuhan, Wuhan 430081, China*
(Received 30 November 2002; published 24 April 2003)

Magnetic and structural properties of $ErMn_6Sn_{6-x}Ga_x$ ($x=0-2.0$) with the $HfFe_6Ge_6$-type structure have been investigated. The compounds ($x=0.2-2.0$) are characterized by ferrimagnetic ordering, and Curie temperatures increase from 75 K for $x=0$ to 383 K for $x=0.4$ and then decrease to 288 K for $x=2.0$, which are due to the contraction of the unit cell and the decrease of conduction-electron density with Ga substitution. The compounds ($x=0.2-2.0$) display large coercive fields ($0.73 \leqslant \mu_0 {}_i H_c \leqslant 2.2$ T) at 5 K. The sign of the second-order crystalline electric-field (CEF) coefficient A_2^0 of the Er sublattice reverses by a small amount of Ga substitution for Sn. Moreover, the fourth-order CEF coefficient A_4^0 of the Er sublattice and sixth-order Stevens factor γ_J are proved to play important roles in the determination of the easy magnetic direction.

DOI: 10.1103/PhysRevB.67.134423 PACS number(s): 75.30.Gw, 75.50.Gg, 75.50.Vv

The magnetic structures and magnetic properties of hexagonal $HfFe_6Ge_6$-type (space group $P6/mmm$) RMn_6Sn_6 (R=Mg, Zr, Hf, Sc, Y, Gd-Tm, Lu) have been studied extensively.[1–7] All these compounds are composed of R and Mn layers alternately stacked along the c axis. The magnetic structures are characterized by ferromagnetic (001) Mn planes with moments lying in the basal plane. The interlayer Mn-Mn coupling is always ferromagnetic through the Mn-Sn-Sn-Sn-Mn slab while the Mn moments arrangement within the Mn-(R,Sn)-Mn slab depends on the nature of the R elements. Previous studies have revealed that these Mn-Mn interlayer interactions are strongly related to the R valence,[3,4] and it is suggested that some significant effects of magnetic properties may be produced by a change of the Sn sites valence.

Recently, we have noticed that large magnetocrystalline anisotropy appears in $RMn_6Sn_{6-x}T_x$ and $RMn_6Ge_{6-x}T_x$ (R: rare-earth elements and T=Ga, In) compounds.[8–10] Those studies have suggested that the magnetocrystalline anisotropy is mainly driven by the fourth-order Stevens coefficient in the germanides and by the second-order one in the stannides.[8,9] In order to better understand these behaviors, we decided to investigate the structural and magnetic properties of the $ErMn_6Sn_{6-x}Ga_x$ ($0 \leqslant x \leqslant 2.0$) compounds.

$ErMn_6Sn_{6-x}Ga_x$ polycrystalline samples were synthesized by arc melting the constituent elements in a highly purified Ar atmosphere, and then annealing at 750 °C for 10 days in an evacuated quartz tube. After the heat treatment, x-ray-diffraction (XRD) studies were carried out using a Rigaku Rint 1400 diffractometer with Cu K_α radiation. The XRD patterns indicate all the $ErMn_6Sn_{6-x}Ga_x$ ($0 \leqslant x \leqslant 2.0$) compounds crystallize to a $HfFe_6Ge_6$-type structure with a minor impurity of Mn_3Sn_2. The cell parameters of all the samples are listed in Table I. Due to the smaller ionic radius of Ga compared with that of Sn, the substitution leads to a decrease of the cell parameters a and c. However, the ratio of c/a is constant for all the samples, indicating an isotropy contraction. The Mn-Mn interatomic distances between layers are proportional to the lattice constant c. So the decrease of the lattice constants by the substitution of Ga for Sn means the reduction of the interatomic distances of Mn atoms, both within and between the layers. A Rietveld study of the XRD data[11] was carried out for the $ErMn_6Sn_4Ga_2$ compound (see Fig. 1). The refinement result reveals that the Ga atom occupies all the three Sn positions and prefers the $2c$ site (see Table II). The site occupancies of $ErMn_6Sn_4Ga_2$ are not in agreement with those of $ErMn_6Ge_6Ga$ in which the preferential site of Ga is the $2e$ site.[10]

According to the cell parameters and the site occupancies above, we have calculated the total energies of

TABLE I. Structural and magnetic data of the $ErMn_6Sn_{6-x}Ga_x$ compounds.

x	a (nm)	c (nm)	c/a	v(nm^3)	T_C (K)	T_{SR} (K)	J_{MnMn} (10^{-23} J)	μ_{Mn} (5 K) (μ_B)	μ_{Mn} (300 K) (μ_B)
0 [a]	0.5518	0.9007	1.631	0.2373	75			2.2 (4.2 K)	1.31 (this work)
0.2	0.5508	0.8990	1.632	0.2362	379	36	20.9	2.38	1.72
0.4	0.5470	0.8973	1.632	0.2348	383	56	21.3	2.42	1.73
0.8	0.5485	0.8954	1.632	0.2333	376	106	21.2	2.43	1.75
1.0	0.5473	0.8927	1.631	0.2315	360	156	20.4	2.34	1.68
1.5	0.5450	0.8881	1.630	0.2284	342	227	19.5	2.35	1.62
2.0	0.5343	0.8710	1.630	0.2154	288	247		2.37	

[a]References 5 and 6.

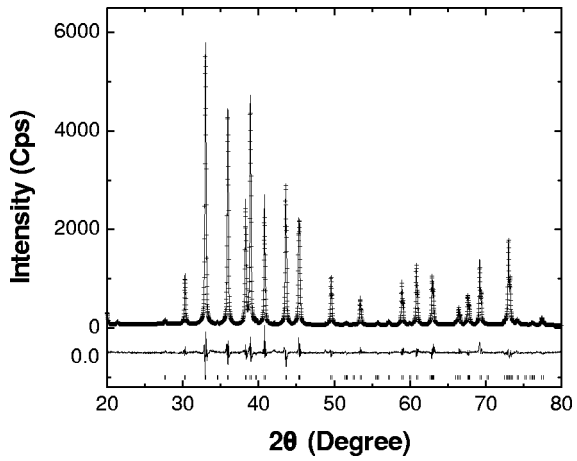

FIG. 1. Observed (solid lines) and calculated (crosses) XRD patterns for $ErMn_6Sn_4Ga_2$. Positions for the Bragg reflection are marked by vertical bars. Differences between the observed and the calculated intensities are shown.

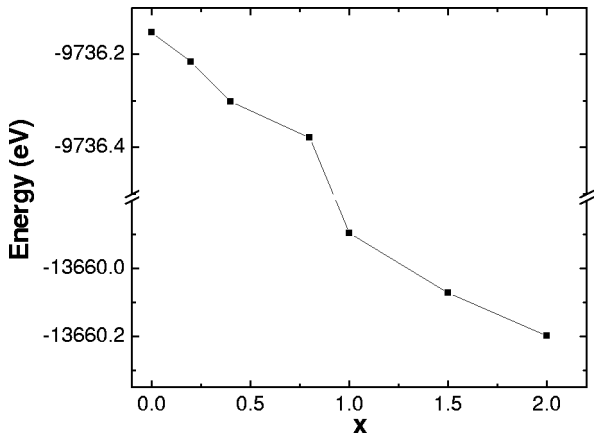

FIG. 2. Calculated variation of the total energies for the $ErMn_6Sn_{6-x}Ga_x$ compounds.

$ErMn_6Sn_{6-x}Ga_x$ ($0 \leqslant x \leqslant 2.0$) using a total-energy pseudopotential method based on generalized gradient approximations in the density-functional theory.[12] The result reveals that the total energies of $ErMn_6Sn_{6-x}Ga_x$ ($0 \leqslant x \leqslant 2.0$) decrease monotonously with increasing content of Ga (see Fig. 2), suggesting that the substitution leads to the stabilization of the formation of $HfFe_6Ge_6$-type compounds.

The magnetization measurement on all the samples was carried out in the temperature range of 5–400 K using a superconducting quantum interference device magnetometer with a maximum field of 50 kOe. The temperature dependence of the magnetization for powder $ErMn_6Sn_{6-x}Ga_x$ ($0 \leqslant x \leqslant 2.0$) samples measured in 0.5 kOe after zero-field cooling is shown in Fig. 3. It is interesting that compounds ($0.2 \leqslant x \leqslant 2.0$) display ferrimagnetic behaviors in the magnetic ordering temperature range. The values of the Curie temperature T_C increase at first from 75 K for $x=0$ (Refs. 5 and 6) to 383 K for $x=0.4$, and then decrease markedly for larger Ga content. For RMn_6Sn_6 compounds ordered at relatively high temperature owing to strong ferromagnetic Mn-Mn intrasublattice exchange,[1] the variation of T_C can be explained by the Mn-Mn interaction using the mean-field model.[13] It is reasonable to neglect the Er-Er interaction relative to Er-Mn and Mn-Mn interactions at high temperatures. Therefore, the exchange-coupling parameter J_{MnMn} can be deduced by the following expression:

$$J_{\mathrm{MnMn}} = \frac{3k_B T_{\mathrm{Mn}}}{2Z_{\mathrm{MnMn}} G_{\mathrm{Mn}}}, \tag{1}$$

where G_{Mn} [$G_{\mathrm{Mn}} = S_{\mathrm{Mn}}(S_{\mathrm{Mn}}+1)$] is the de Gennes factor for the Mn atom, Z_{MnMn} represents the number of Mn nearest neighbors of a Mn ion, and T_{Mn} is derived from the Curie temperatures of $YMn_6Sn_{6-x}Ga_x$ ($0.2 \leqslant x \leqslant 1.8$).[7] The values of J_{MnMn} are given in Table I. For $ErMn_6Sn_{6-x}Ga_x$ compounds, J_{MnMn} should be the sum of the three different magnetic exchange interactions: a direct ferromagnetic J_0 interaction within the (001) Mn planes, and two Mn-Mn superexchange interactions J_1 within the Mn-Sn-Sn-Sn-Mn slab and J_2 within the Mn-(R,Sn)-Mn slab mediated via the polarization of the conduction electrons. The decrease of Mn-Mn interatomic distances, especially the Mn-Mn distance along the c axis, may strengthen the exchange coupling to some extent. Another reason might be related to the change of electronic structure. For the valence-electron configurations of Sn and Ga as free atoms, $4d^{10}5s^2p^2$ and $3d^{10}4s^2p^1$, respectively, the substitution of Ga for Sn decreases the conduction-electron density of the system. The interlayer interactions J_2 and J_3, which are mediated by indirect superexchange via the conduction electrons, like the Ruderman-Kittel-Kasuya-Yosida interaction, can be weakened by the change of conduction-electron density.

For $x=0.2$, an abrupt change in the M-T curve around 36 K is due to the spin reorientation (see Fig. 3). It can be proved by the M-H curves of a magnetically aligned sample

TABLE II. Refined structural parameters of $ErMn_6Sn_4Ga_2$ at room temperature (space group $P6/mmm$).

Atom	Position	x	y	z	Occupancy
Er	1*b*	0	0	0.5	1.00
Mn	6*i*	0.5	0	0.259	1.00
Sn/Ga	2*e*	0	0	0.164	0.75/0.25
Sn/Ga	2*d*	0.333	0.667	0.5	0.72/0.28
Sn/Ga	2*c*	0.333	0.667	0	0.53/0.47
	$a=0.5343$ nm	$c=0.8710$ nm	$v=0.2154$ nm^3		
	$R_P=9.35\%$	$R_{WP}=12.09\%$	$S=1.80$		

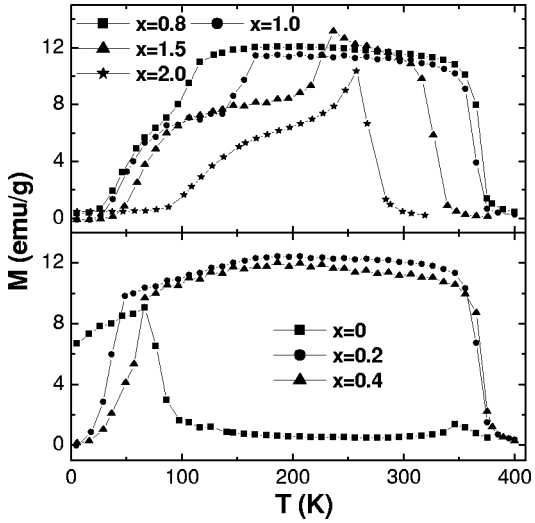

FIG. 3. Temperature dependence of magnetization for the $ErMn_6Sn_{6-x}Ga_x$ compounds in an applied field of 0.5 kOe.

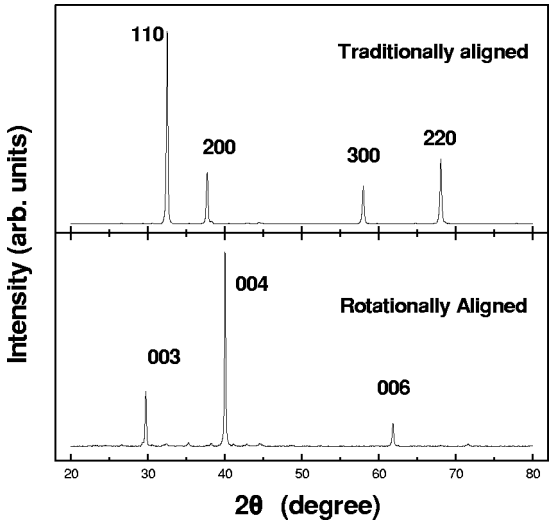

FIG. 5. XRD patterns of the traditionally and rotationally aligned $ErMn_6Sn_{5.8}Ga_{0.2}$ samples.

(see Fig. 4). The $(hk0)$-type and $(00l)$-type peaks are dominant in the patterns of the traditionally aligned sample and the rotationally aligned one, respectively (see Fig. 5). It is evidenced that the easy magnetic direction (EMD) has to be in the *ab* plane at room temperature, in agreement with the EMD of RMn_6Sn_6 at high temperatures.[1] Magnetic measurements were carried out with applied field parallel and perpendicular to the aligned direction for the rotationally aligned sample. While the *ab* plane is the EMD at 60 K, it turns into the hard magnetic direction (HMD) at 5 K (see Fig. 4). Therefore, it is reasonable to assume that the spin reorientation exists between 5 and 60 K. The same measurements have been carried out for $ErMn_6Sn_5Ga$, and it is verified that the EMD changes from the *c* axis to the *ab* plane between 125 and 180 K. So, it is believed that the magnetic moments of all the samples ($0.2 \leqslant x \leqslant 2.0$) rotate from the *ab* plane to the *c* axis with decreasing temperature. The temperatures of the spin reorientation, T_{SR}, are gathered in Table I, and are elevated monotonously with Ga content. The values indicate that the introduction of Ga strengthens the character of the axial magnetocrystalline anisotropy for the $ErMn_6Sn_{6-x}Ga_x$ compounds.

Figure 6 shows isothermal magnetization curves for powder samples with variation of applied field at 5 K and 300 K. At 300 K, the magnetization curve displays a metamagnetic behavior for $ErMn_6Sn_6$ with a threshold field of 10 kOe. For the samples with $0.2 \leqslant x \leqslant 1.5$, the magnetization increases relatively faster at low fields and approaches saturation at high fields, indicating their ferrimagnetic character. The sample with $x = 2.0$ exhibits a linear variation of the *M*-*H* curve, corresponding to the paramagnetic state ($T_C < 288$). It is noticeable that all the samples ($0.2 \leqslant x \leqslant 2.0$) displays discontinuous magnetization curves at low fields at 5 K, espe-

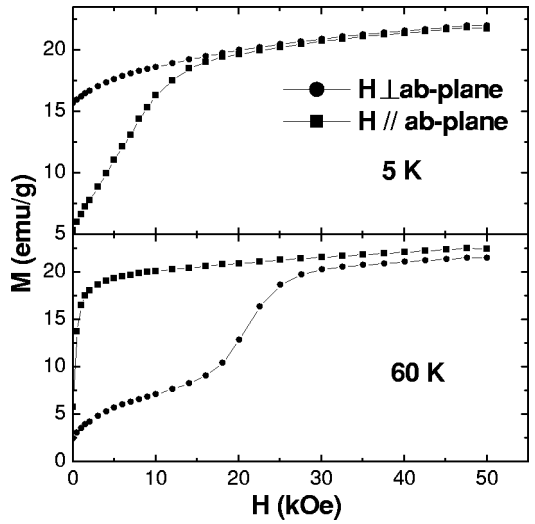

FIG. 4. Magnetization curves of the rotationally aligned $ErMn_6Sn_{5.8}Ga_{0.2}$ sample with the field applied perpendicular and parallel to the *ab* plane at 60 K and 5 K. The external magnetic field is applied from 5 T to 0.

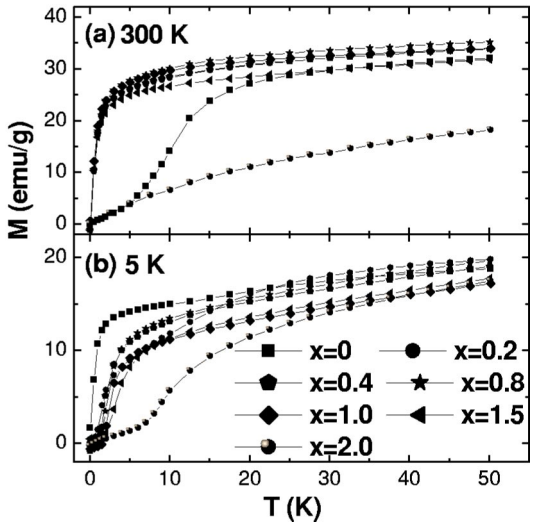

FIG. 6. Magnetic-field dependence of magnetization for the $ErMn_6Sn_{6-x}Ga_x$ powder samples at 5 and 300 K.

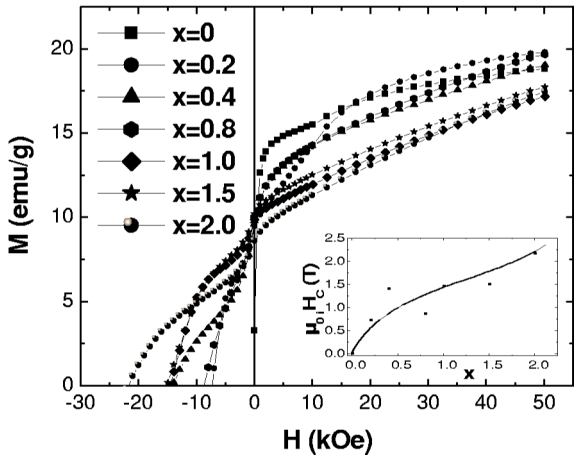

FIG. 7. Magnetization of the $ErMn_6Sn_{6-x}Ga_x$ powder samples as a function of applied fields at 5 K. The inset displays the variation of coercive fields $\mu_{0\ i}H_c$ with Ga concentration.

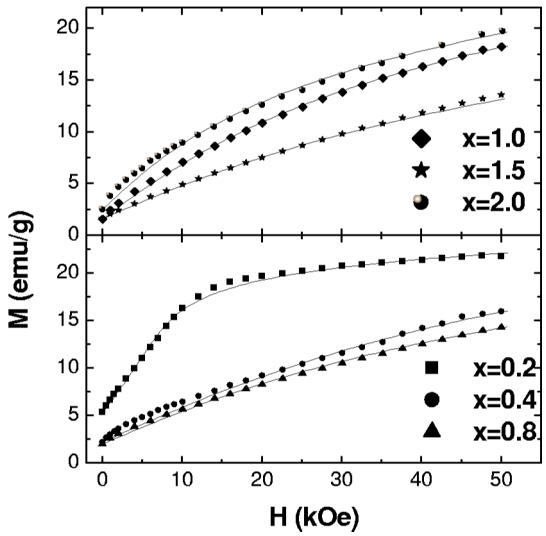

FIG. 8. Experimental (symbols) and calculated (solid lines) magnetization curves of the rotationally aligned $ErMn_6Sn_{6-x}Ga_x$ samples measured perpendicular to the *c* axis at 5 K.

cially for $x=2.0$ [see Fig. 6(b)]. This variation is not related to a metamagnetic transition from an antiferromagnetic arrangement to a ferrimagnetic one, but it can be considered as the first-order magnetization process with a considerable contribution of high-order magnetocrystalline anisotropy terms. This is discussed in detail below. The saturation moments of the Mn atoms are derived by extrapolating the *M*-*H* curves to $H=0$, and we adopt the values of $9.4\mu_B$ at 5 K and $2.41\mu_B$ at 300 K measured for $ErMn_6Ge_5Ga$ as the moment of Er^{+3}.[10] The temperature dependence of the magnetic moment of Er^{+3} for $ErMn_6Ge_5Ga$ is shown in Ref. 10. These moments of Mn atoms are slightly larger than those ($2.20\mu_B$ at 4.2 K and $1.31\mu_B$ at 300 K) for $ErMn_6Sn_6$ (see Table I), which might arise from variations in the Mn 3*d*-band overlap due to the decrease of the Mn-Sn(Ga) interatomic distance and the decrease of free-electron density.

It is very interesting to find large coercive fields in the *M*-*H* curves for the compounds ($0.2 \leqslant x \leqslant 2.0$) at 5 K (see Fig. 7). For $ErMn_6Sn_6$, easy-planar magnetization is exhibited in the whole magnetic ordering temperature range[6] and coercive field can be seldom observed (0.17 kOe at 5 K). However, the sample with $x=0.2$ presents large coercive fields (0.74 kOe at 5 K) indicating easy-axial magnetic behavior, in good agreement with the EMD along the *c* axis at low temperature proved by the isothermal magnetization measurement for the aligned sample above (see Fig. 4). The values of the coercive fields increase with Ga content, and even reach a magnitude of 21.8 kOe with $x=2.0$ (see the inset of Fig. 7).

To better understand the evolution of the magnetocrystalline anisotropy with the Ga content for these compounds ($0.2 \leqslant x \leqslant 2.0$) at low temperature, we have investigated the magnetization process for the oriented samples. All the XRD patterns of the oriented samples are fairly similar to those of $ErMn_6Sn_{5.8}Ga_{0.2}$ in that the $(hk0)$-type and $(00l)$-type peaks are dominant for the traditionally aligned and the rotationally aligned samples, respectively (see Fig. 5). It is obvious that the EMD has to be in the *ab* plane at room temperature and along the *c* axis at 5 K. In order to obtain the magnetocrystalline anisotropy constants K_1 and K_2, the isothermal magnetization curves of rotationally aligned samples were measured by applying the field perpendicular to the *c* axis at 5 K with a decreasing field model (see Fig. 8). Considering the misalignment of the EMD and the total free energy composed of the crystalline anisotropy energy and the magnetostatic energy for the oriented samples, the magnetic field *H* and the component of magnetization *M* parallel to *H* are given by

$$H=\frac{2K_1\sin\theta\cos\theta+4K_2\sin^3\theta\cos\theta}{\mu_0 M_S\sum_i\ [P_i\cos(\xi_i+\theta)]}, \tag{2}$$

$$M=M_S\sum_i\ [P_i\sin(\xi_i+\theta)], \tag{3}$$

where θ represents the angle between the spontaneous magnetization M_S and the EMD, and $P_i=P_0\exp(-2\xi_i^2/\varpi^2)$ denotes a Gaussian distribution of the *c* axis around the aligning direction of grain *i* where ξ_i is the angle between the EMD and the aligning direction of grain *i*, ϖ is the degree of misalignment, and P_0 is a normalization constant.[14] So, the experimental *M*-*H* curves in the HMD direction for the aligned samples can be perfectly fitted with Eqs. (2) and (3) by using the angle distribution, which is shown in Fig. 8, and the values of constants K_1 and K_2 are depicted in Fig. 9. For the samples, the anisotropy constants *K* are the sum of K_{Er} and K_{Mn} which are the anisotropy constants of the Er sublattice and Mn sublattice, respectively. Since the magnetocrystalline anisotropy of the rare-earth sublattice is preponderant at low temperature for RMn_6Sn_6,[1] it is reasonable to take no account of the anisotropy contribution of the Mn sublattice, i.e., $K=K_{Er}$ at 5 K.

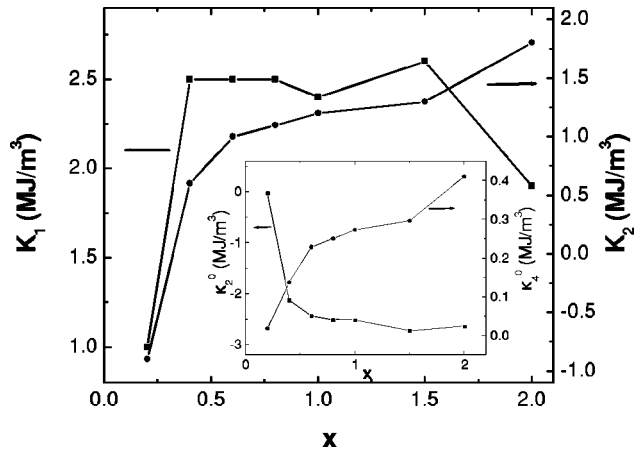

FIG. 9. Composition dependence of magnetocrystalline anisotropy constants K_1 and K_2 of the $ErMn_6Sn_{6-x}Ga_x$ compounds. The inset shows the composition dependence of magnetocrystalline anisotropy coefficients $\varkappa_2^0$ and $\varkappa_4^0$.

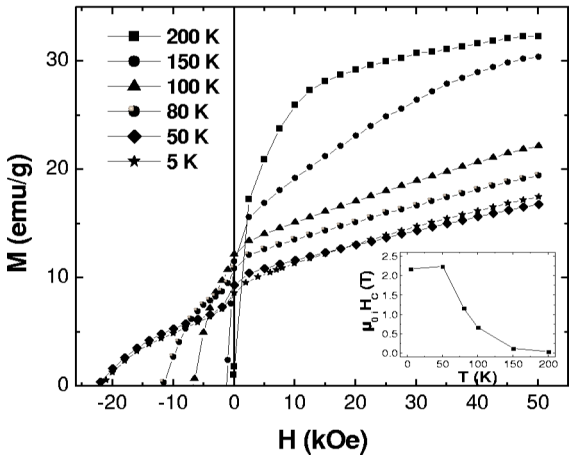

FIG. 10. Magnetization of the $ErMn_6Sn_4Ga_2$ powder sample as a function of applied fields at various temperatures. The inset displays the thermal variation of coercive fields $\mu_{0\ i}H_c$.

In the single-ion anisotropy theory, a simple relationship between the anisotropy constants K_n and the anisotropy coefficients χ_n^m for the hexagonal symmetry can be given by Eqs. (4) and (5):[15]

$$K_1 = -\tfrac{1}{2}(3\varkappa_2^0 + 10\varkappa_4^0 + 21\varkappa_6^0), \tag{4}$$

$$K_2 = \tfrac{1}{8}(35\varkappa_4^0 + 189\varkappa_6^0). \tag{5}$$

Assuming the sixth-order coefficient $\varkappa_6^0 = 0$, the variations of coefficients $\varkappa_2^0$ and $\varkappa_4^0$ are shown in the inset of Fig. 9. It is well known that the relations between the coefficients $\varkappa_n^m$ and the crystalline electric-field (CEF) parameters B_n^m can be expressed as

$$\varkappa_n^m = B_n^m \langle O_n^m \rangle, \tag{6}$$

where $\langle O_n^m \rangle$ denotes the expectation values of the Stevens operators of order n. The CEF parameters B_n^m can be written as

$$B_n^m = \theta_n \langle r_{4f}^n \rangle A_n^m, \tag{7}$$

where θ_n represents the Steven facotrs α_J, β_J, and γ_J, and $\langle r_{4f}^n \rangle$ is the mean value of the nth power of the $4f$ shell radius, which depends only on the nature of the rare-earth atoms.[15] For $ErMn_6Sn_{6-x}Ga_x$ ($0 \leqslant x \leqslant 2.0$), the defining factor is the CEF coefficients A_n^m which are determined by the electrostatic potential due to the environment. For the $ErMn_6Sn_6$ compound, the Er atom in the center is surrounded by six Sn atoms at the $2d$ site, two Sn atoms at the $2e$ site, and 12 Mn atoms at the $6i$ site. According to the XRD analysis of $ErMn_6Sn_4Ga_2$ above (see Fig. 1 and Table II), it is clear that the Ga atoms replace Sn at all three Sn positions, especially at the $2d$ and $2e$ sites, which changes the coordination configuration of the Er atom. For RMn_6Sn_6 compounds, the negative B_2^0 parameter leads to an easy-axis magnetocrystalline anisotropy in the R sublattice and the positive one induces an easy-plane behavior.[6] Since the substitution of Ga for Sn decreases the conduction-electron density of the system, it makes the coefficients A_2^0 negative and A_4^0 positive, from which the negative B_2^0 and the positive B_4^0 parameters can be derived by Eq. (7) while B_2^0 is positive in $ErMn_6Sn_6$.[6] The absolute values of A_2^0 and A_4^0 increase with shorter Er-Sn(Ga) distances and decrease the conduction-electron density of the system, which gives rise to the change of the anisotropy coefficients $\varkappa_2^0$ and $\varkappa_4^0$ with Ga content. Therefore, the uniaxial magnetocrystalline anisotropy behavior of the compounds is reinforced by the introduction of Ga. The result is in good agreement with the fact that the anisot-

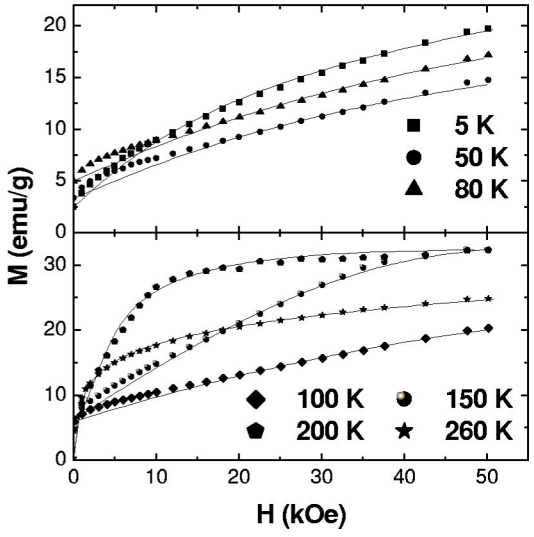

FIG. 11. Experimental (symbols) and calculated (solid lines) magnetization curves of the rotationally aligned $ErMn_6Sn_4Ga_2$ sample with the applied field perpendicular to the EMD at various temperatures. The EMD is in the *ab* plane at 260 K and is along the *c* axis at other temperatures.

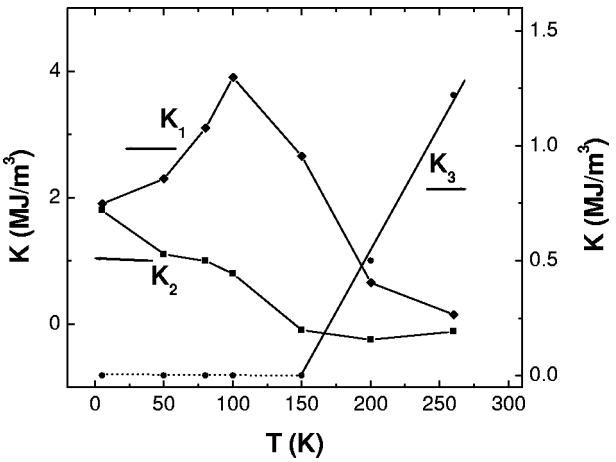

FIG. 12. Temperature dependence of magnetocrystalline anisotropy constants K_1, K_2, and K_3 for $ErMn_6Sn_4Ga_2$.

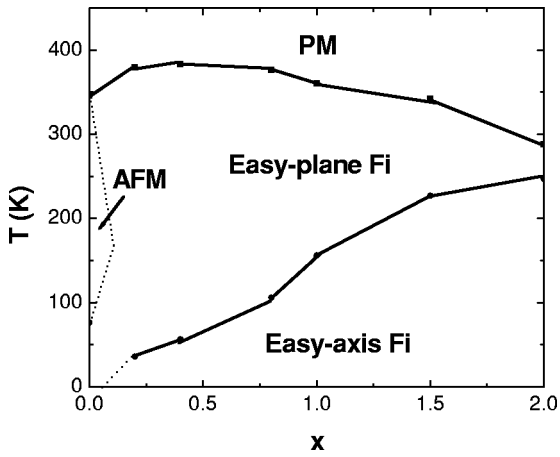

FIG. 13. X-T magnetic phase diagram for the $ErMn_6Sn_{6-x}Ga_x$ compounds. Fi, AFM, and PM represent ferrimagnetism, antiferromagnetism, and paramagnetism, respectively. The magnetic state in the dotted region of the figure is ambiguous.

ropy behavior of RMn_6Sn_6 is determined not only by the second-order parameter A_2^0, but also by the parameters of order higher than A_2^0.[2]

In order to clarify the magnetic hardness with temperature variation, the isothermal magnetization curves for the $ErMn_6Sn_4Ga_2$ powder sample with applied field from 5 T to coercive field at various temperatures were recorded in Fig. 10. The compound maintains a rather large coercive field of about 2.2 T in the range 5–50 K, and decreases from 2.25 T at 50 K to 0.04 T at 200 K (see the inset of Fig. 10). The M-H curves of the rotationally aligned sample with applied field parallel to the HMD at various temperatures are shown in Fig. 11 and are fitted by Eqs. (2) and (3). The temperature dependence of K_1 and K_2 is shown in Fig. 12. With increasing temperature, the contribution of the third-order anisotropy constant K_3 has to be considered and the value of K_3 even reaches 1.22 MJ/m^3 at 260 K (see Fig. 12). This is because the easy-planar character is reinforced by the Mn sublattice with increasing temperature and the easy-plane anisotropy is dominant when higher than the temperature of spin reorientation ($T_{SR}=247$ K). This is compatible with the fact that the EMD within the basal plane is governed by the sixth-order Stevens factor γ_J for RNi_5 compounds.[15] The temperature dependencies of the anisotropy coefficients of the Mn sublattice may be obtained from studies of the magnetic anisotropy of $RMn_6Sn_{6-x}T_x$ (R=Y, Lu, Sc; T=Ga, In) or $GdMn_6Sn_6$.

In summary, the evolution of magnetic properties for the $ErMn_6Sn_{6-x}Ga_x$ compounds with Ga content is shown in the x-T magnetic phase diagram (see Fig. 13). According to the studies on $RMn_6Sn_{6-x}In_x$ (R=Er, Tm) in which the In-poor compounds display reentrant ferrimagnetism,[8] it should be interesting to examine the magnetic properties of the weakly substituted $ErMn_6Sn_{6-x}Ga_x$ ($0<x<0.2$) compounds (dotted region in Fig. 13). This investigation reveals that the substitution of Ga for Sn plays an important role in the magnetocrystalline anisotropy. The Er sublattice displays considerable easy-axial behavior arising from the positive CEF coefficient A_2^0. The fourth-order CEF coefficient A_4^0 and sixth-order Stevens factor γ_J play some role in the determination of the easy-axis magnetic direction at low temperatures and the easy-plane magnetic direction at high temperatures for the compounds, respectively. Moreover, it is particularly interesting to examine the evolution of the magnetocrystalline anisotropy in $RMn_6Sn_{6-x}Ga_x$ (R=Gd, Tm) compounds since R sublattices of RMn_6Sn_6 (R=Gd, Tm) are characterized by easy-plane behaviors in the whole range of magnetic ordering temperature.

This work was supported by the State Key Project of Fundamental Research and National Natural Sciences Foundation of China. We would like to thank Professor Tong-yun Zhao and Dr. Chang-min Xiong for helpful discussions.

*Email address: roger@g203.iphy.ac.cn

[1] B. Chafik Ei Idrissi, G. Venturini, B. Malaman, and D. Fruchart, J. Less-Common Met. **175**, 143 (1991).
[2] M.W. Dirken, R.C. Thiel, J.H.V.J. Brabers, F.R. de Boer, and K.H.J. Buschow, J. Alloys Compd. **177**, L11 (1991).
[3] T. Mazet, G. Venturini, R. Welter, and B. Malaman, J. Alloys Compd. **264**, 71 (1998).
[4] T. Mazet, R. Welter, and B. Malaman, J. Alloys Compd. **284**, 54 (1999).
[5] D.M. Clatterbuck, R.J. Lange, and K.A. Gschneidner, Jr., J. Magn. Magn. Mater. **195**, 639 (1999).
[6] B. Malaman, G. Venturini, R. Welter, J.P. Sanchez, P. Vulliet, and E. Ressouche, J. Magn. Magn. Mater. **202**, 519 (1999).
[7] S.Y. Zhang, P. Zhao, Z.H. Cheng, R.W. Li, J.R. Sun, H.W. Zhang, and B.G. Shen, Phys. Rev. B **64**, 212404 (2001).
[8] C. Lefevre, G. Venturini, and B. Malaman, J. Alloys Compd. **329**, 76 (2001).
[9] C. Lefevre and G. Venturini, J. Alloys Compd. **334**, 45 (2002).
[10] C. Lefevre, G. Venturini, and B. Malaman, J. Alloys Compd. **335**, 26 (2002).

[11] R.A. Young, A. Sakthivel, T.S. Moss, and C.O. Paiva-Santos, J. Appl. Crystallogr. **28**, 366 (1995).
[12] M.C. Payne, M.P. Teter, D.C. Allan, T.A. Arias, and J.D. Joannopoulos, Rev. Mod. Phys. **64**, 1045 (1992).
[13] K.H.J. Buschow, Rep. Prog. Phys. **54**, 1123 (1991).
[14] H.S. Li and B.P. Hu, J. Phys. Colloq. **49**, 513 (1998).
[15] J. J. M. Franse and R. J. Radwanski, *Handbook of Magnetic Materials*, edited by K. H. J. Buschow (North-Holland, Amsterdam, 1993), Vol. 7.